878–892 Nucleic Acids Research, 2010, Vol. 38, No. 3 Published online 24 November 2009
doi:10.1093/nar/gkp1011

Transcription regulation of caspase-1 by R393 of HIPPI and its molecular partner HIP-1

M. Banerjee[1,2], M. Datta[1,2], P. Majumder[1], D. Mukhopadhyay[2] and N. P. Bhattacharyya[1,2,*]

[1]Crystallography and Molecular Biology Division and [2]Structural Genomics Section, Saha Institute of Nuclear Physics, 1/AF Bidhan Nagar, Kolkata 700 064, India

Received June 13, 2009; Revised August 26, 2009; Accepted August 31, 2009

ABSTRACT

Earlier we have shown that exogenous expression of HIPPI, a molecular partner of Huntingtin interacting protein HIP-1, induces apoptosis and increases expression of caspases-1, -8 and -10 in HeLa and Neuro2A cells. The C-terminal pseudo death effector domain of HIPPI (pDED-HIPPI) specifically interacts with the putative promoter sequences of these genes. In the present manuscript, we predict from structural modeling of pDED-HIPPI that R393 of HIPPI is important for such interaction. R393E mutation in pDED-HIPPI decreases the interaction with the putative promoter of caspase-1 in cells. Expression of caspase-1 is decreased in cells expressing mutant pDED-HIPPI in comparison to that observed in cells expressing wild type pDED-HIPPI. Using HIP-1 knocked down cells as well as over expressing HIP-1 with mutation at its nuclear localization signal and other deletion mutations, we demonstrate that translocation of HIPPI to the nucleus is mediated by HIP-1 for the increased expression of caspase-1. HIPPI-HIP-1 heterodimer is detected in cytoplasm as well as in the nucleus and is associated with transcription complex in cells. Taking together, we are able to show the importance of R393 of HIPPI and the role of HIPPI-HIP-1 heterodimer in the transcription regulation of caspase-1.

INTRODUCTION

HIPPI (HIP-1 protein interactor), also known as ESRRBL1 (estrogen-related receptor beta like 1), a homolog of Chlamydomonas intraflagellar transport 57 (IFT57), does not have any known domain except a 'pseudo death effector domain' (pDED) and a myosin like domain (MLD). Interaction of HIPPI with HIP-1 is through the pDED, specifically through 409 K, present in the putative helix5 of HIPPI-pDED, although other regions might have influence on such interactions (1). HIPPI-HIP-1 heterodimer recruits procaspase-8 and activates the initiator caspase and its downstream apoptotic cascades (1,2). It has been shown earlier that the strength of interaction of HIP-1 with Huntingtin (HTT) protein, whose mutation causes Huntington's disease (HD), is inversely correlated with the number of glutamines (Q) at the N-terminal region of HTT (3). It is proposed that weaker interaction of HIP-1 with mutated HTT in HD might increase the freely available pool of HIP-1 and might, in turn, enhance the propensity of hetero-dimerization of HIP-1 with HIPPI. The elevated pool of HIPPI-HIP-1 complex may then recruit procaspase-8 and lead to increased cell death as observed in HD (1,2).

In addition to increased apoptosis by the activation of different caspases, truncation of Bid, release of AIF from the mitochondria, endogenous expressions of caspase-1, -3, -7 and -8 are also increased in GFP-Hippi expressing Neuro2A and HeLa cells, whereas mitochondrial genes ND1, ND4 and anti-apoptotic gene Bcl-2 are down regulated (2). We have subsequently shown that HIPPI can directly interact both *in vitro* and *in vivo* with a 60 bp sequence (−151 to −92) upstream of the caspase-1 gene. HIPPI, especially its C-terminal pDED, interacts with the specific sequence motif AAAGACATG (−101 to −93) present at the promoter sequence of caspase-1 (4,5). Similar motifs are also present at the putative promoter sequences of caspase-8 and caspase-10. HIPPI interacts with these promoters and increases the expression of these genes (5). This result indicates that HIPPI, without having any known DNA-binding domain,

*To whom correspondence should be addressed. Tel: +91 33 2337 5345/49; Fax: +91 33 2337 4637; Email: nitai_sinp@yahoo.com or nitaipada.bhattacharya@saha.ac.in
Present address:
Pritha Majumder, Department of Cancer Genetics, Roswell Park Cancer Institute, Elm & Carlton Street, Buffalo, NY 14263, USA.

The authors wish it to be known that, in their opinion, the first two authors should be regarded as joint First Authors.

interacts with DNA and regulates transcription. Specific amino acid(s) that interact with the DNA sequence still remains unknown. Besides, the question of nuclear translocation of cytoplasmic HIPPI for transcription regulation, without having classical nuclear localization signal (NLS) is yet to be resolved.

HIP-1, the molecular partner of HIPPI interacts with membranes, traffics endocytic vesicles and translocates into the nucleus using its own NLS at the C-terminus (6) and has been implicated in cancer (7). HIP-1 interacts directly with androgen receptor (AR), accumulates in the nucleus upon androgen stimulation and recruits to DNA elements regulated by AR. AR also translocates to the nucleus in response to androgen and the process is facilitated by HIP-1 (6,8,9). HIP-1 thus regulates the transcription of AR responsive genes through its interaction with AR. Given that HIP-1 can act as the nuclear transporter for AR and regulate the expressions of its target genes, we tested the hypothesis that HIPPI might also be translocated to the nucleus assisted by HIP-1 and could regulate the expression of caspase-1 gene.

MATERIALS AND METHODS

Antibodies and other reagents

RNase A, BSA, Geniticin, Hygromycin, DAPI, Hoechst, nuclei isolation kit, anti-Beta-actin (A2228, clone AC-74, Lot number: 107K4791) antibody and Protein G were obtained from Sigma Chemicals (MO, USA). Assay kit for detection of caspase-8 activation was obtained from Alexis Biochemicals, Switzerland. The anti-mouse and anti-rabbit secondary antibodies conjugated with horseradish peroxidase, TRITC and FITC conjugated antibodies were purchased from Bangalore Genei, India; anti-GFP antibody was purchased from BD Biosciences, USA (632375, Lot number: B7040316); anti-histone 2B (H2B) antibody (IMG-359 Lot number: 073101A) and anti-caspase-1 antibody (IMG-804-4, Lot number: AB093004A) were from Imgenex, USA; anti-HIP-1 was purchased from Novus Biologicals (NB300-204, 1B11, Lot number: A); and anti-HIPPI antibody (ab5205-100, Lot number: 63362) and anti-LaminB antibody (ab16048-25, Lot Number 393854) were purchased from Abcam, USA. Immobilon-P Transfer membrane was from Millipore, USA, Chemilumiscence kit from Pierce, USA, *Taq polymerase* from Bioline, USA, and restriction enzymes (BamHI, SalI, SmaI, XhoI and HindIII) were from Promega, USA. Protease inhibitor cocktail was purchased from Roche, USA. Other molecular biology grade fine chemicals were procured locally.

Methods for modeling and prediction for DNA-binding property

Comparative structure-based modeling was done using MODELLER 8v1 (10) with a multiple structural alignment template, generated by CEMC (11) using 3D co-ordinates of all DED containing proteins (CATH homologous super family 1.10.533.10) (12) from PDB (13). Out of twenty energy-minimized models, one with the minimum objective function was chosen for generating accessible molecular surface with electrostatic potential map using GRASP (14). Prediction of DNA-binding property was made using PreDs, by submitting the coordinates of modeled pDED of HIPPI and its mutant protein via the online tool using default parameters (http://pre-s.protein.osaka-u.ac.jp/~preds/). The tool makes prediction of dsDNA-binding site on protein surfaces. The prediction for the query protein is made based on the value of the prediction score, $P_{score,}$ which is a vectorial property of the surface and an indicator of the ratio of the predicted area (P_{area}) to the whole area on the protein surface. The protein with a higher P_{score} than 0.12 is considered as a dsDNA-binding protein.

Construction of clones

Constructions of GFP-Hippi and GFP-pDED (coding for 335 to 429 amino acids of HIPPI) have been described earlier (2,5). The HIP-1 clone in pcDNA3 (pcDNA3 Hip-1) was kindly provided by Prof. T.S Ross, University of Michigan Medical School, USA. The mutant HIP-1 containing a glutamic acid (E) at the position 58 and 1005 (designated as Hip-1 58E and Hip-1 1005E) clones in pcDNA3 were kindly provided by Dr. Ian Mills, CRUK Uro-Oncology Research Group, Cambridge, CB2 0RE, UK. Full length Hip-1, N terminus Hip-1 (Hip-1N, 1–258aa) and pDED of Hip-1 (Hip-1P, 410–491aa) were sub-cloned in DsRed C1 vector. The details of the primer sequence, PCR condition and restriction enzymes used are shown in the Table 1.

Site directed mutagenesis

A mutation [replacing the Arginin (R) residue at 393 position of HIPPI (59th position of pDED of HIPPI), by Aspartic acid (E) residue (AGA to GGA)] was introduced in GFP-pDED of HIPPI by PCR directed site-specific mutagenesis with GFP-pDED as a template. The recombinant GFP-pDED was subjected to PCR-directed mutagenesis using mutagenic oligonucleotide primers containing mismatch bases. The mutagenic PCR involved the generation of two PCR products that overlap in sequence containing the same mutation introduced as part of the PCR primers. A subsequent re-amplification of these fragments with cloning primers as described earlier (5) resulted in the enrichment of the full-length pDED-HIPPI.

MutR59EF: 5′-GACATT**ga**AATTGGCATTGTGG-3′
MutR59ER: 5′-GCCAATT**tc**AATGTCCATCT-3′

The mutation thus introduced was confirmed by sequencing. The plasmid harboring the mutated gene was designated as GFP-mpDED.

Cell culture and transfection

HeLa and Neuro2A cells were routinely grown in MEM (HIMEDIA, India) while K562 cells were grown in RPMI (HIMEDIA, India) supplemented with 10% fetal bovine serum (Biowest, USA) at 37°C in 5% CO_2 atmosphere under humidified condition.

Transfection of cells was performed using Lipofectamine 2000 (Invitrogen, USA). Unless otherwise

Table 1. Primer sequences for construction of various clones of Hip-1

Clone name	Primer sequences	Condition	RE sites	Host plasmid
DsRed-Hip-1	5′-ACGCGTCGACCATGAGAAAGG-3′ 5′-AGGGGGCCCCGGTTACCACTT-3′	95°C → 5 min [95°C 30 s, 50°C 30 s 72°C 120 s] × 32 cycles 72°C → 10 min	SalI SmaI	DsRed-C1
DsRed-Hip-1N	5′-CCGCTCGAGATGGATCGGATGGCCAGC-3′ 5′-ACGCGTCGACCCCGGTGGCCTTGCAGGGTG-3′	95°C → 5 min [95°C 30 s, 55°C 30 s, 72°C 120 s] × 32 cycles 72°C → 10 min	XhoI SalI	DsRed-C1
DsRed-Hip-1P	5′-ACGC*GTCGAC*AGCGAGCTGGAAGCAGAT-3′ 5′-CG*GGATCC*CTCTGCATTCTTCCGCAGCA-3′	95°C → 5 min [95°C 30 s, 65°C 30 s, 72°C 60 s] × 35 cycles 72°C → 10 min	SalI BamH1	DsRed-C1

mentioned, for single transfection experiment 2 μg (60 mm plate) or 5 μg (100 mm plate) of DNA constructs as well as 7 or 15 μl of Lipofectamine 2000 respectively were used. For co-transfection, equal amount of DNA constructs (5 μg each for 100 mm plate) were used. After 24 h, transiently transfected cells were checked for transfection efficiency by monitoring GFP or DsRed expression under fluorescence microscope and were used for experiments. Transfection efficiency varied from 70 to 90%.

To generate cell lines that stably express wild type and mutant HIP-1, Neuro2A cells were grown in 100 mm plates to ~30% confluency. Cells were then transfected using 5 μl of Lipofectamine 2000 and 2 μg of the required plasmid [pcDNA3Hip-1, Hip-1 1005E, Hip-1 58E]. Transfected cells were then selected using G418 (final concentration 0.4 mg/ml). After 10–15 days, clones were pooled and grown in the presence of G418. Before the experiment selection was withdrawn and used for the studies.

Knockdown of HIP-1 in HeLa and Neuro2A cells by siRNA

DNA sequences 779-ACCGCTTCATGGAGCAGTTTA-799 and 1394-ACAGCGATATAGCAAGCTAAA-1415 of human Hip-1 (gi|38045918|ref|NM_005338.4|) were designed for the siRNAs using the online software from GenScript (https://www.genscript.com/ssl-bin/app/rnai). The scrambled sequence (5′-TAGTCGCATACGGAAC ATTCG-3′) for the first siRNA was also designed using GenScript sequence scrambler tool. The complete sequence which was inserted into the expression vector pRNATin-H1.2/Hygro was 5′-TAAACTGCTCCATGA AGCGGTTTGATATCCGACCGCTTCATGGAGCAG TTTATTTTTTCCAA-3′ (designated Hip1Si) with termination signal and appropriate restriction site linkers (BamH1 and HindIII, not shown) and an insert for loop formation (underlined). Similarly for a second siRNA to target the human Hip-1 the complete sequence 5′-TTTAG CTTGCTATATCGCTGTTTGATATCCGACAGCGA TATAGCAAGCTAAATTTTTTCCAA-3′ (designated as Hip1Si1) was cloned as above. The entire sequence for the scramble siRNA was 5′-CGAATGTTCCGTATGCGA CTATTGATATCCGTAGTCGCATACGGAACATTC GTTTTTTCCAA-3′ (designated as Hip1Scr). The cloned fragments were sequenced and confirmed. The cloned DNA fragments (Hip1Si and Hip1Si1) were purchased from GeneSript, USA and the Hip1Scr was cloned in our laboratory using the restriction enzymes BamH1 and HindIII. The purchased clones were further checked with the recommended restriction enzymes (BamH1 and HindIII) digestion and used for our experiments. Mouse HIP-1 (gi|22122460|NM_146001) sequences contain a single mismatch (410-ACCGCTTCATGGAG CAGTT**C**A-430 of mouse HIP-1) compared with that of in human (779-ACCGCTTCATGGAGCAGTT**T**A-799).

HIP-1 siRNA clones and the scramble siRNA were transfected in HeLa cells using Lipofectamin2000 (Invitrogen, USA) using protocol provided by the manufacturer. Transfected cells were selected for Hygromycin resistance. Colonies grown in presence of Hygromycin were pooled and grown to sufficient numbers for protein isolation and other experiments. Protein was isolated and western blot analysis was carried out using anti HIP-1 antibody. Similarly for Neuro2A cells, Hip1Si was transfected to knock down HIP-1. Similar down regulation of HIP-1 was observed in spite of a single mismatch in siRNA sequence. In parallel, HeLa cells were also transfected with the empty vector (pRNATin-H1.2/ Hygro, without the insert) and selected for Hygromycin resistance and used to check the expression of HIP-1. No change in the expression of HIP-1 was observed with cells expressing the empty vector. In all our experiments, we have used HeLa cells or Neuro2A cells as the control, while studying the effect of HIP-1 (in knocked down cells).

Detection of apoptosis by nuclear fragmentation and caspase-8 activation

Nuclear fragmentation and caspase-8 activation were detected using the methods described earlier (2). In brief, cells were grown on cover slips, washed thrice with PBS and fixed with 1:1 mixture of methanol and acetone (1 h at 4°C). Cells were then stained with 1 mM Hoechst in phosphate buffer saline (PBS) in the dark at room temperature for 5 min and observed under a fluorescence microscope (Olympus BX60 with appropriate attachment, Japan). Cells with intact nuclear morphology (normal)

and fragmented nuclei (apoptotic cells) were determined and the percentage of cells with apoptotic nuclei was calculated. About 200–500 cells were counted for each experiment. Activation of caspase-8 was determined according to the protocols provided by the manufacturers of the kit. Exponentially growing 2 million HeLa cells expressing GFP–wpDED and GFP-mpDED were collected and processed as mentioned earlier (2). For the caspase-8 detection, the fluorescence of liberated AFC was measured at its emission maxima (λ_{max} 505 nm) with the excitation at the 400 nm.

Confocal microscopy

Cells were grown on cover slips overnight and were washed with PBS, fixed with 1:1 mixture of methanol and acetone, stained with 4′,6-diamino-2-phenylindole (DAPI; final concentration 10 μg/ml) and mounted on clean glass slides using 1–2 μl of glycerol. The cells were visualized under confocal microscope (Zeiss LSM 510) and the localization of GFP tagged and DsRed tagged proteins were observed by exciting at 488 and 543 nm, respectively. Subsequent fluorescence was monitored at 503 nm and 583 nm respectively using LSM 510 software.

Sub-cellular fractionation, immunoprecipitation and western blot analysis

Cells grown in 100 mm Petri dishes were washed with ice cold PBS and harvested at 300*g* for 3 min at 4°C. The pellet was suspended in cytosol extraction buffer (50 mM Tris–Cl pH 7.5, 10 mM NaCl, 2 mM EDTA, 1 mM PMSF and 1× protease inhibitor cocktail) and kept on ice for 15–20 min. Cells were then lysed by adding 0.25% NP-40 and centrifuged immediately at 800*g* for 5 min at 4°C. The supernatant was kept as cytosolic extract. The pellet was then suspended in nuclear extraction buffer (50 mM Tris–Cl pH 7.5, 400 mM NaCl, 2 mM EDTA, 1 mM PMSF and 1× protease inhibitor cocktail) and kept on ice for 40 min followed by centrifugation at 13 000*g* for 20 min at 4°C. The supernatant was kept as nuclear extract. For immunoprecipitation assay with cytosolic and nuclear extract, cytosolic extract was prepared as described above. Nucleus was isolated by resuspending the nuclear pellet in nuclear IP buffer (50 mM Tris–HCl pH 7.5, 150 mM NaCl, 2 mM EDTA, 1 mM PMSF and 1× protease inhibitor cocktail) followed by repeated freezing and thawing and centrifugation at 13 000*g* for 20 min at 4°C. The extracts are then incubated with anti HIP-1 antibody (1:200 dilutions) for 2 h at 4°C. Next BSA soaked protein-G agarose was added to the reaction mix and incubated over night at 4°C under continuous rotating condition. Next day the immunoprecipitated complex was collected by centrifugation at 1000*g* for 2 min at 4°C. Beads were washed twice with nuclear IP buffer, once with wash buffer I (50 mM Tris–Cl pH 7.5, 400 mM NaCl, 2 mM EDTA, 1 mM PMSF and 1× protease inhibitor cocktail) and finally with wash buffer II (50 mM Tris–Cl pH 7.5, 400 mM NaCl, 2 mM EDTA, 0.1% Triton X-100, 1 mM PMSF and 1× protease inhibitor cocktail). The bound proteins were extracted from beads by boiling with SDS gel loading buffer and were subjected to western blot using anti HIPPI and anti HIP-1 antibody. The methods used for western blot analysis was essentially the same as described earlier (2).

For immunoprecipitation assay using whole cell extract, cells grown in 10 cm Petri dishes were washed in ice cold PBS and harvested at 300*g* for 3 min at 4°C. The pellet was suspended in co-immunoprecipitation buffer (50 mM Tris–Cl pH 7.5, 15 mM EDTA, 100 mM NaCl, 0.1% Triton X-100 and PMSF with 100 μg/ml final concentrations), lysed by freezing and thawing and centrifuged at 13 000*g* for 15 min. The supernatant was collected and protein was estimated. To detect GFP tagged proteins, immunoprecipitation with anti-GFP antibody (1:500 dilutions) was carried out using the protocol described above. The beads were washed several times with co-immunoprecipitation buffer and the precipitated complex was extracted from beads by boiling with SDS gel loading dye. Western blot analysis was performed using anti-GFP, anti-caspase-8 and anti-HIP-1 antibodies. For other proteins, western blot analysis was carried out using anti HIP-1; anti HIPPI, anti-GFP, anti-H2B, anti Lamin B and anti Beta actin antibodies after standardizing for appropriate dilutions. Beta actin was used as internal control for cytoplasmic extract while H2B or lamin B was used for loading controls for proteins in the nuclear fractions. Each experiment was repeated 2–3 times. Integrated optical density (IOD) of each band was calculated using Image Master VDS software (Amarsham Biosciences, UK). When ever necessary, IOD was normalized with that of the loading control.

Immunocytochemistry

Cells were grown on cover slips and transfected with respective constructs whenever necessary as described above. Cells (after 24 h of transfection, for transfected cells) were fixed with 3.7% freshly prepared Paraformaldehyde for 20 min at room temperature, washed thrice with PBS, and permeabilized with 0.1% Triton X-100 in PBS for 10 min at room temperature. It was then rinsed thrice with PBS and blocked in 2% BSA for 1 h. The coverslips containing cells were then incubated for 1 h at 37°C with primary antibodies (anti HIP-1, anti HIPPI) with (1:50) dilutions. Cells were then washed thrice with PBS and incubated with fluorophore-conjugated (FITC or TRITC) secondary antibodies at 37°C in dark. Cover slips were again washed with PBS and then mounted on slides. Photographs were taken using (ZEISS LSM 510) confocal microscope.

Chromatin immunoprecipitation (ChIP) and re-chromatin immunoprecipitation (reChIP) assay

Methods used for the ChIP experiments were adapted from the results published earlier (2). GFP-wpDED or GFP-mpDED transfected HeLa cells and K562 were grown on petri plates to 80–90% confluency as mentioned above. Cells were incubated with 2% formaldehyde for 2 min at room temperature to cross-link the proteins with the DNA. This cross-linking reaction was stopped using 150 mM Glycine. Cells were scraped and spun

down at 300 g for 2 min, washed twice with PBS and the pellet was frozen in dry ice for 20 mins. Buffer C (20 mM HEPES (pH 7.9), 25% glycerol, 420 mM NaCl, 1.5 mM $MgCl_2$, 0.2 mM EDTA) with 1 mM PMSF was added to the pellet after thawing at 4°C to lyse the cells. Nuclei were spun down at 15 000 g for 10 min and the pellet was re-suspended in breaking buffer (50 mM Tris–HCl pH 8.0, 1 mM EDTA, 150 mM NaCl, 1% SDS and 2% Triton X-100) and sonicated twice (two pulses of 10 s each). Contents were then spun down. The pellet was discarded. Triton buffer (50 mM Tris–HCl pH 8.0, 1 mM EDTA, 150 mM NaCl and 0.1% Triton X-100) was added to the supernatant (nuclear extract). Anti-GFP (for GFP-pDED transfected HeLa cells) or anti-HIPPI (for K562 cell) antibody was added to a part of the nuclear extract (+Ab) and antibody reaction was carried out overnight at 4°C. Other part of the nuclear extract was kept at 4°C (−Ab). The next day Protein G Agarose beads were added to the +Ab and −Ab fractions and left on a shaker for 6 h at 4°C. After 6 h, beads were washed 4 times with Triton buffer and two times with Tris buffer [10 mM Tris–HCl (pH 8.0)].

Next SDS–NaCl–DTT buffer (62.5 mM Tris–HCl, pH 6.8, 200 mM NaCl, 2% SDS 10 mM DTT) was added to the beads and incubated at 65°C overnight for reverse cross-linking. Next day, all the fractions were subjected to phenol chloroform extraction and the aqueous layer was collected. Cross-linked DNA was precipitated with 3 M Sodium acetate and ethanol. DNA pellet was washed with 70% ethanol, dried and then dissolved in distilled water. The DNA so obtained was amplified by PCR using caspase-1 717 bp upstream sequences (4). The primer sequences (5′–3′) were as follows:

Forward: 5′-GGAAGATCTGGCTTTTCTCTCTCCCTTC-3′
Reverse: 5′-CGGGGTACCAAGCCTAGGAAACACAAGGAGA-3′

For re-ChIP assay, HeLa cells grown in 10 cm Petri dishes to ~80–90% confluency were transfected with GFP-Hippi construct. After 24 h, transfection efficiency was monitored by fluorescence microscopy and was ~80%. The cells were then cross-linked and the first immunoprecipitation using anti HIPPI antibody was carried out as described above. The immunoprecipitated chromatin was then eluted from beads using ChIP elution buffer (50 mM Tris–HCl, pH 7.5, 10 mM EDTA, 1% SDS) and incubating at 68°C for 10 min. One part of the eluted chromatin was subjected to reverse cross-linking followed by phenol chloroform isolation of DNA as mentioned above to check the first immunoprecipitation. The other part of the eluted DNA-protein complexes was diluted with Triton buffer and incubated with anti HIP-1 antibody over night at 4°C. Next day, the DNA-protein-antibody complex was immunoprecipitated by adding Protein G Agarose beads and DNA was extracted by phenol chloroform isolation followed by ethanol precipitation. PCR amplification of the eluted DNA was carried out using caspase-1 upstream (300 bp) sequence specific primers. The primer sequences (5′–3′) were as follows:

Forward: 5′AATGATTGAGAAACTCTTCACTGTGT-3′
Reverse: 5′-CGGGGTACCAAGCCTAGGAAACACAAGGAGA-3′

Real-time PCR

RNA (100 ng) was reverse transcribed as described earlier (2). Real-time RT–PCR reaction was carried out using Sybr green 2× Universal PCR Master Mix (Applied Biosystems, USA) in ABI Prism 7500 sequence detection system. Each reaction was performed in triplicate using primer sequences for caspase-1 (2). Non-template control reaction at the same condition was performed to ascertain the baseline and threshold value for the analysis. C_t value obtained for caspase-1 was normalized with respect to beta actin (ΔCt). Differences between the ΔCt values of test and control sets were determined (ΔΔCt). The fold change was determined using the formula $2^{-\Delta\Delta Ct.}$

Statistical analysis

All the experiments were done at least two times. Statistical analysis, mainly unpaired *t*-test, whenever necessary was carried out using the on-line software GraphPad QuickCalc available at http//www.graphpad.com/quickcalcs/ttest1.cfm

RESULTS

Modeling of pDED of HIPPI: possible residues involved in the interaction with DNA

It has been shown earlier by us that pDED of HIPPI (pDED-HIPPI) interacts with the putative promoter sequence of caspase-1 (4,5). To interact with DNA, pDED therefore requires a complimentary surface and appropriate charge distribution on its interfaces. Amino acid similarity of pDED-HIPPI with other DEDs (mainly DNA-binding DED, known as DEDD) or any other DNA-binding proteins did not provide any clue about the surface charge property. Pseudo Death Effector Domains (pDED) of HIP-1 and HIPPI share 39.2% similarity and 26.6% identity whereas pDED-HIPPI has 34.9% similarity and 21% identity with other DEDs (1). To test the hypothesis that pDED-HIPPI might have DNA-binding surface/groove, theoretical structural model building for pDED was done using standard procedures. The available surface of the model was compared with the modeled structure of pDED of HIP-1 (pDED-HIP-1) (15) and the crystallographically determined (2.8 Å) structure of DED of FADD (DED-FADD) (16). Within the predictable limit of theoretical model building and on the basis of the assumptions made by Gervais and co workers (1) in defining the pDED, the modeled domain expectedly took up an orthogonal six helix bundle conformation with rmsd (for Cα superposition) values 1.26 Å and 0.9 Å for pDED-HIPPI and pDED-HIP-1 respectively, despite a sequence homology of only ~14% with their nearest neighbors. However, only pDED-HIPPI showed a positively charged trough on its surface (Figure 1B, shown in blue colour), probably fit for binding a linear stretch of DNA molecule. In case of pDED-HIP-1 (Figure 1B), the trough was only incompletely formed with partial charge complimentarity. Generally, DED containing proteins do

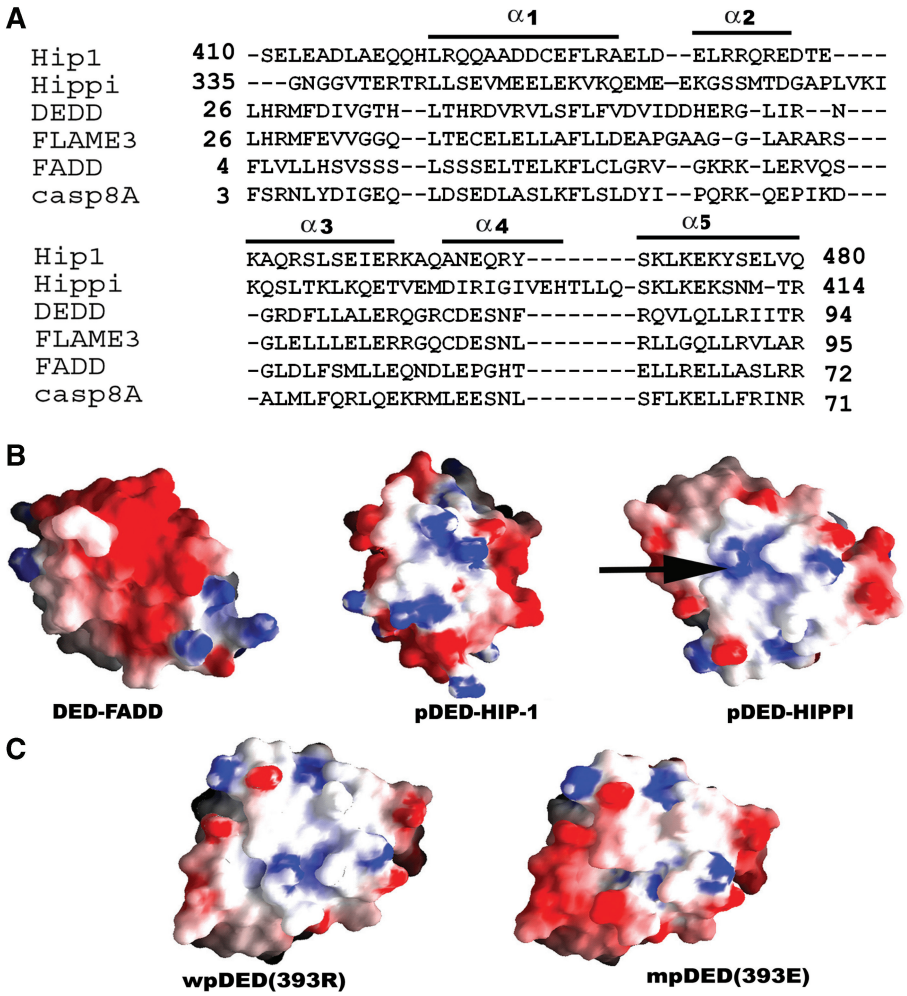

Figure 1. Alignment of DED like domains of different proteins and modeling of pDED of HIPPI and its mutant. (**A**) Amino acid sequence alignment of DED like domains of HIP-1, HIPPI, DEDD, FLAME3, FADD and caspase-8A. N-terminal regions of the domains up to helix α5 are shown. Predicted helices are taken from published data (1). (**B**) Electrostatic surface potential of crystal structures of DED-FADD (PDB Id: 1a1w) and theoretical models of pDED-HIP-1 and pDED-HIPPI. Front view of the surface constituted by helices α1, α3, and α4 is shown. A putative DNA-binding trough on pDED-HIPPI is marked by arrow (positive charge potential is shown in blue). Same region for pDED of HIP-1 formed partially complimentary surface for putative DNA-binding region whereas that of DED of FADD takes a different topology with negatively charged surface. (**C**) Model structures of wild type pDED of HIPPI with R393 and its mutant E393. In spite of having similar topology in both the cases, they differ in surface charge distribution.

not possess such a characteristic surface (Figure 1B, DED-FADD) whereas DNA-binding DEDD proteins form similar surface (17), with a few basic residues present at the similar region in their primary structures (Figure 1A). A closer look on wild type pDED-HIPPI model [Figure 1C, wpDED (393R)] revealed that this surface was constituted by helices α1, α3 and α4 and the surface positive charge was contributed mainly by the side-chains of R393, K384 and K382 of HIPPI residing on α4 (positions R59, K50 and K48 of pDED). We shall henceforth follow the amino acid numbering for the HIPPI only. It was observed further that *in silico* mutation of R393 to E393 destroyed the electrostatic surface that might help in DNA recognition [Figure 1C, mpDED (393E)]. These modeling studies indicated that mutation at any of these residues on the DNA-binding interface formed by the helices α1–α3–α4 might lead to the loss of putative DNA-binding function of pDED-HIPPI.

We also used PreDs, a prediction tool for proteins to bind with double stranded DNA (http://pre-s.protein.osaka-u.ac.jp/~preds/), for checking the probable ability of the wild type pDED-HIPPI (with R393) and for its mutant form (with E393) to interact with DNA. The score of this prediction (P_{score} = 0.13) was significant for the wild type pDED-HIPPI revealing that the wild type domain may interact with DNA. The P_{score} for the mutant pDED-HIPPI was 0.05, indicating that the mutant protein is unlikely to interact with DNA. Interestingly, pDED-HIP-1 also provided an insignificant score (P_{score} = 0.06) showing a lack of DNA-binding propensity. PreDs prediction further supported this observation in modeling studies described above.

Mutant pDED-HIPPI (R393E) is unable to interact with caspase-1 promoter and increase caspase-1 expression

We tested whether R393E mutation altered caspase-1 expression and DNA binding of pDED-HIPPI. We cloned both wild type (R393) and mutated (E393) pDED-HIPPI in pEGFP vector and expressed in HeLa cells. These clones are denoted by wpDED and mpDED respectively. Expressions of mpDED and wpDED were similar as revealed by western blot analysis and confocal microscopy (Figure 2A and B). Immunoprecipitation with anti-GFP antibody and detection by anti-HIP-1 antibody (Figure 2C, upper panel) revealed that both mutated and wild type pDED interacted with endogenous HIP-1, similar to that obtained with full length HIPPI (1,2).

We then tested whether mpDED altered the expression of caspase-1 in comparison to that observed with wpDED. Real time PCR using caspase-1 gene specific primers was carried out using mRNA isolated from HeLa cells expressing wpDED and mpDED. Results shown in Figure 2F revealed that the mutation R393E significantly decreased the caspase-1 gene expression by about 22 fold ($n = 3$, $P = 0.001$) in comparison to that obtained in cells expressing wild type pDED-HIPPI. Unlike caspase-1 expression, nuclear fragmentation and caspase-8 activation were not decreased significantly in mpDED cells in comparison to that obtained with wpDED cells. Nuclear fragmentation increased significantly in GFP-wpDED ($P = 0.0001$, $n = 2$) and GFP-mpDED ($P = 0.0016$, $n = 2$) expressing cells in comparison to that obtained in parental HeLa cells (Figure 2G). Similar significant increase in caspase-8 activation ($P = 0.0001$, $n = 2$) for cells expressing wild type or mutated pDED-Hippi was obtained. It is also to be noted that the ability of pDED-HIPPI to induce nuclear fragmentation ($P = 0.03$, $n = 2$) and caspase-8 activation ($P = 0.005$, $n = 2$) were significantly lower in comparison to that obtained with full length HIPPI (comparing Figure 2G and 3H). This data showed that the full length HIPPI induced apoptosis more than that of pDED-HIPPI as has already been shown earlier (1). Percent of cells containing nuclear fragmentation in mpDED was (26 ± 5) whereas this value was (32 ± 2) in wpDED cells (Figure 2G). This difference was not statistically significant ($P = 0.14$). Activation of caspase-8 (Figure 2G) was also similar ($P = 0.2$). These results showed that the mutation R393E of pDED-HIPPI decreased the expression of caspase-1. However its ability to induce apoptosis remains unaltered.

We then tested whether the mpDED could interact with the caspase-1 promoter sequence *in vivo* as has been shown with full-length HIPPI earlier by ChIP assay (4). The result (Figure 2H) obtained in this experiment showed that even though the wild type pDED was able to interact with the caspase-1 upstream sequence (Figure 2H, panel I), the mutant pDED was unable to do the same (Figure 2H, panel II). It confirmed our prediction from the modeling study that the R393 of HIPPI was indeed involved in the interaction with the caspase-1 promoter sequence.

Role of HIP-1 in the increased expression of caspase-1 gene and apoptosis

In HeLa cells, considerable level of endogenous HIP-1 is present without any detectable HIPPI expression (2). To check whether HIP-1 played any role in enhanced expression of caspase-1, endogenous HIP-1 was knocked down in HeLa cells by expressing specific siRNA cloned in pRNA Tin-H1.2/Hygro (denoted by 'Hip1Si', see 'Materials and Methods' section for detail). To nullify the possibility of any off target effect of the siRNA, a scramble siRNA (Hip1Scr) was also transfected in HeLa cells. Stable transfections with the siRNA reduced the expression of HIP-1. Result of a typical experiment is shown in the Figure 3A and the average IOD of independent experiments is shown in Figure 3B. Average expression of HIP-1 was reduced significantly ($P = 0.0001$, $n = 5$) to 0.37 in Hip1Si transfected cells compared to that in HeLa cells (normalized IOD = 1) while expression of the scramble siRNA reduced the expression of HIP-1 slightly but was not statistically significant ($P = 0.54$, $n = 3$, Supplementary Figure S3).

To check further the specificity of HIP-1 down regulation by the Hip1Si, we transiently transfected the wild type Hip-1 cloned in pcDNA3 in stably transfected Hip1Si cells (denoted by Hip1SiHip1 in Figure 3C). HIP-1 expression in these cells was significantly higher ($P = 0.013$, $n = 3$) compared to the cells where HIP-1 was knocked down (Figure 3C and 3D). This result shows that the Hip-1Si specifically down regulates the expression of HIP-1.

To study the effect of HIP-1 on caspase-1 expression, we transiently transfected GFP-Hippi in HeLa as well as in stably transfected Hip1Si cells (designated as 'Hippi' and 'Hip1SiHi' respectively) and compared the expression of caspase-1 by western blot analysis (Figure 3E). It was evident that caspase-1 expression was decreased significantly ($n = 3$, $P = 0.0091$) in 'Hip1SiHi' cells compared to that observed in 'Hippi' cells. When GFP-Hippi and pcDNA3 Hip-1 was transiently transfected in cells stably expressing Hip1Si, the expression of HIP-1 was lower than that of the parental HeLa cells, while higher than Hip1Si cells. Such increase in HIP-1 expression in HIP-1 knocked down cells also increased the expression of caspase-1 (Figure 3E, middle panel and Figure 3G). As described above, this result shows that the Hip1Si specifically down regulates the expression of HIP-1 (Figure 3F) and HIP-1 up regulates the expression of caspase-1.

Transient expression of GFP-Hippi in cells with reduced HIP-1 ($\sim$0.37 of the endogenous expression) significantly decreased nuclear fragmentation ($P = 0.0001$) and caspase-8 activation ($P = 0.0001$) as shown in Figure 3H. In summary, the above observations indicated that HIP-1 is playing an important role in HIPPI mediated transcription of caspase-1 and apoptosis induction by HIPPI.

Translocation of HIPPI into the nucleus requires expression of HIP-1

To investigate the role of HIP-1 on sub-cellular distribution of HIPPI, we transiently transfected GFP-Hippi in HeLa and Hip1Si cells and visualized under confocal

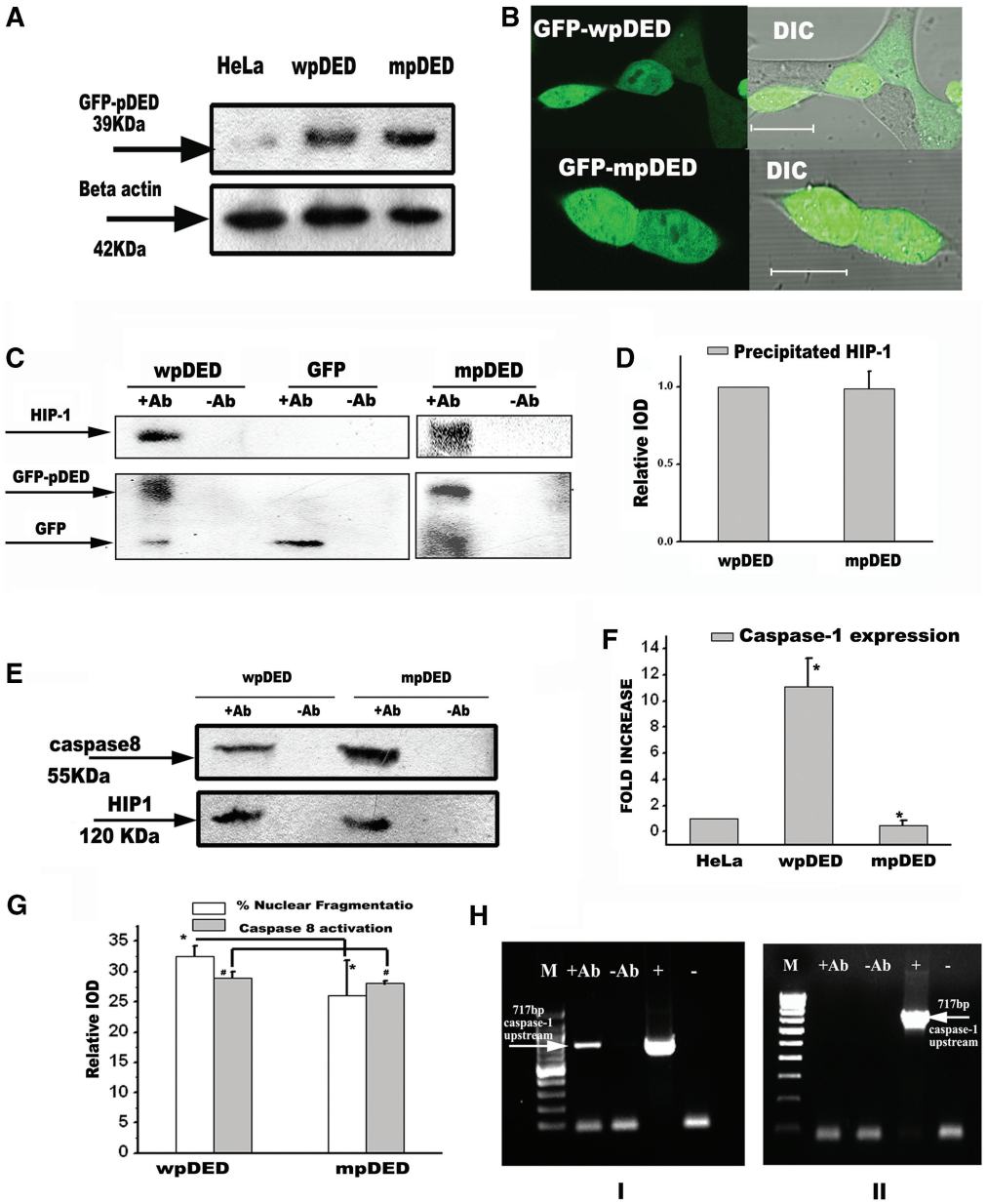

Figure 2. Expressions of wild type and mutated GFP-pDED-HIPPI, their interactions with endogenous HIP-1 and influences on caspase-1 expression. (**A**) Western blot analysis with total cell extracts from parental HeLa cells (HeLa); wild type GFP-pDED expressing HeLa cells (wpDED) and mutated GFP-(R393E) pDED expressing HeLa cells (mpDED) using anti GFP antibody. Upper panel represents the result of a typical experiment for expression of exogenous GFP-wpDED and its mutant GFP-mpDED (39 kDa). Lower panel represents 42 kDa band corresponding to β-actin used as loading control. (**B**) Confocal microscopic photographs showing the expression and cellular distribution of wild type GFP–pDED (upper panel) and mutated GFP-pDED (E393) (lower panel) in HeLa cells. White bar represents the dimension of a single cell (50 μm). (**C**) Western blot analysis with immunoprecipitated protein pulled down by anti-GFP antibody from HeLa cells expressing GFP-wpDED ('wpDED'), empty GFP vector ('GFP') and GFP-mpDED ('mpDED'). Upper panel: Lane +Ab represent immunoblot carried out using anti HIP-1 antibody with protein immunoprecipitated by anti-GFP antibody; the band represents 120 kDa HIP-1. Lane −Ab: Immunoprecipitation reaction is carried out similarly in absence of GFP antibody. Lower panel: Same blot was stripped and immunobloted with anti-GFP antibody as control for immunoprecipitation (25 kDa band). (**D**) The bar diagram represents the mean integrated optical density IOD, ($n = 2$) of bands obtained by western blot analysis with anti-HIP-1 normalized by the IOD values obtained with anti-GFP antibody (specification is shown in the Figure). Vertical bar represents the standard deviation. (**E**) Western blot analysis of immunoprecipitated proteins by anti HIP-1 antibody from GFPwpDED and GFPmpDED cells and detection of caspase-8 by anti caspase-8 antibody. Upper Panel: lane +Ab denotes immunoblot carried out with anti caspase-8 antibody from immunoprecipitated proteins from cells mentioned above. Lane −Ab represents immunoprecipitation reaction in absence of anti HIP-1 antibody. Lower panel represents immunobloting with anti HIP-1 antibody as control for immunoprecipitation. (**F**) Expression of caspase-1 in 'mpDED' and 'wpDED' cells by real time PCR using sequence specific caspase-1 primers. Expression of beta actin was taken as control. Significance level is $P = 0.001$ ($n = 3$). (**G**) Nuclear fragmentation (white bar) and caspase-8 activation (grey bars) in 'mpDED' and 'wpDED' cells. Significance levels (P-values) of differences in nuclear fragmentation and caspase-8 activation are 0.14 (*) and 0.2 (#) respectively. (**H**) *In vivo* interactions of wild type pDED and mutated pDED with putative promoter sequence (−700 to +17) of caspase-1 by ChIP assay. PCR amplification was carried out using caspase-1 upstream 717 bp sequence specific primers from immuoprecipitated DNA pulled down by anti-GFP antibody from 'wpDED' (panel I) and 'mpDED' (panel II) cells. Lane M shows the markers, Lanes +Ab shows PCR amplification of immunoprecipitated DNA by anti-GFP anibody, lane −Ab represents PCR amplification with chromatin prepared from the same cell extract using only Rabbit IgG secondary antibody but in absence of anti-GFP antibody, Lane + shows PCR carried out with DNA isolated from HeLa cells, lane − represents no template control for PCR.

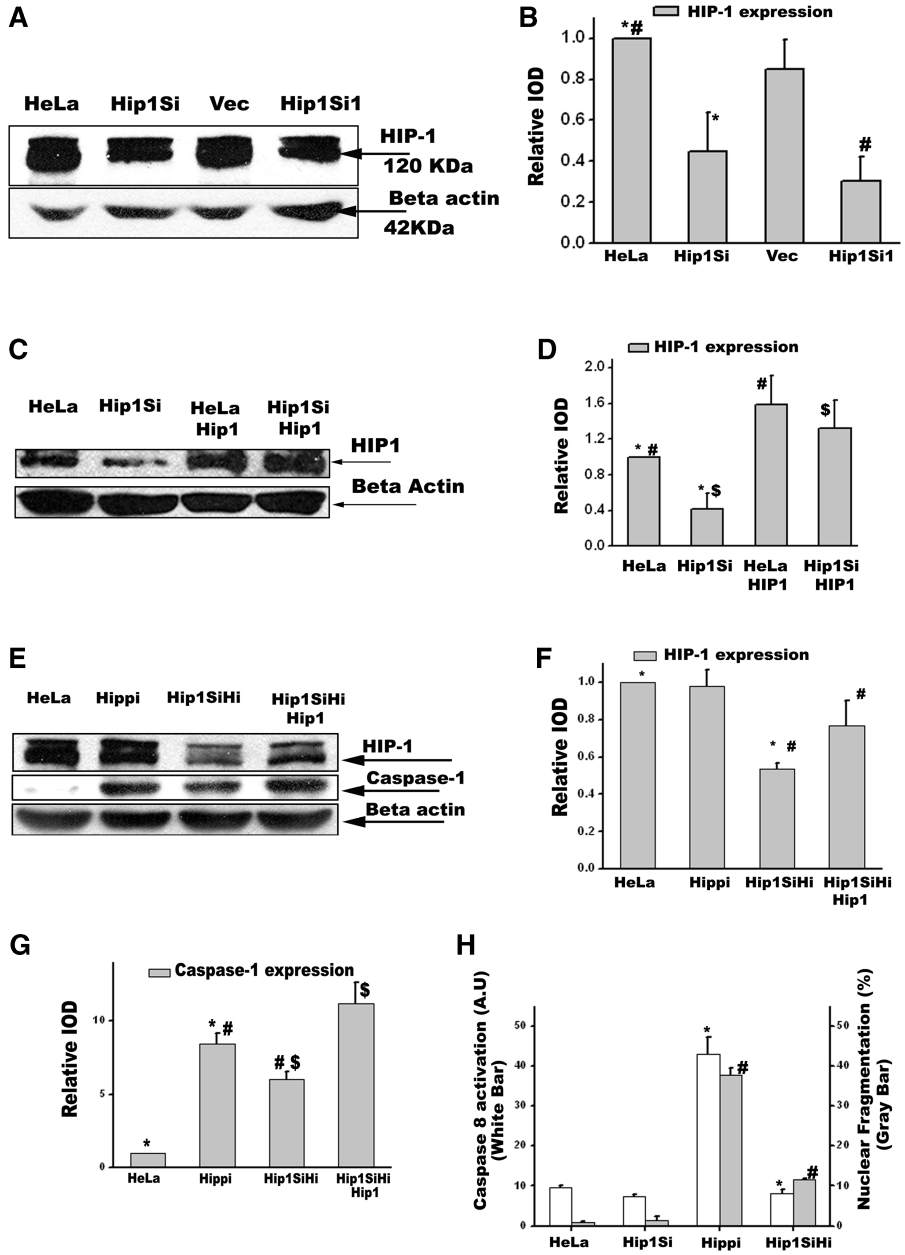

Figure 3. Role of endogenous HIP-1 in increased expression of caspase-1 gene and apoptosis induction by exogenous HIPPI. (**A**) Result of a typical experiment to detect the endogenous expression of HIP-1 by western blot analysis (upper panel) in HeLa cells (designated as HeLa) and HeLa cells stably transfected with Hip1Si construct to knock down HIP-1 (designated as 'Hip1Si'), empty pRNATin-H1.2/Hygro vector (designated as vec) and Hip1Si1 construct, siRNA to target a different region of Hip-1 (designated as 'Hip1Si1'). In the lower panel, the 42 kDa band represents beta actin as loading control. (**B**) The bar diagram represents mean integrated optical densities of bands corresponding to HIP-1 and normalized with that of the loading control beta actin. In each case, the expression of HIP-1 in control HeLa cells was considered to be 1 and the relative expressions of the experimental samples were determined. Level of significance (P) for Hip1Si cells was $P = 0.0001$ ($n = 4$), for Hip1Si1 cells, $P = 0.0011$ ($n = 3$) and for vector transfected cells $P = 0.25$ ($n = 2$) in comparison to that of HeLa cells. (**C**) Western blot analysis for the detection of HIP-1 (upper panel) in parental HeLa cells (HeLa), HeLa cells transfected with Hip1Si construct (Hip1Si), HeLa cells transiently transfected with pcDNA3-Hip1 (HeLaHip1) and Hip1Si cells transiently transfected with pcDNA3-Hip1 (Hip1SiHip1). The lower panel represents 42 kDa band of beta actin as a loading control. (**D**) The bar diagram represents mean integrated optical densities of bands corresponding to HIP-1 and normalized with that of the loading control beta actin. Level of significances (P) are $^{*}P = 0.0006$, $^{\#}P = 0.01$, $^{\$}P = 0.013$. (**E**) Western blot analysis for the detection of HIP-1 (upper panel) and procaspase-1 (middle panel) in HeLa cells ('HeLa'), HeLa cells transiently transfected with GFP-Hippi ('Hippi'), Hip1Si cells transiently transfected with GFP-Hippi ('Hip1SiHi') and Hip1Si cells transiently co-transfected with GFP-Hippi and pcDNA3-Hip-1 ('Hip1SiHiHip1'). Lower panel shows the 42 kDa band corresponding to loading control beta actin. (**F**) Bar diagram showing the mean IOD of bands obtained by western blot analysis ($n = 3$) with anti-HIP-1 antibody relative to the bands obtained for beta actin. Relative expressions of experimental cases were determined by considering the expression in control HeLa cells to be 1. Level of significances (P) are $^{*}P = 0.0001$, $^{\#}P = 0.047$. (**G**) Bar diagram showing the mean relative IOD ($n = 3$) of bands obtained by western blot analysis with anti caspase-1 antibody, normalized with that of loading control beta actin. Relative expressions of experimental cases were determined by considering the expression in control HeLa cells to be 1. Levels of significances between various pairs are indicated by different symbols $^{*}P = 0.0001$, $^{\#}P = 0.009$, $^{\$}P = 0.0045$. (**H**) Bar diagram showing caspase-8 activation by fluoremetric assay (represented by white bars) and percentage of cells containing nuclear fragmentation (grey bars) in 'HeLa', 'Hip1Si', 'Hippi' and 'Hip1SiHi' cells. Various symbols to indicate the paired samples compared are also shown in the figure. The P values are $^{*}P = 0.0001$, $^{\#}P = 0.0001$.

microscope after 24 h (Figure 4A). Result revealed that in HeLa cells GFP-HIPPI was distributed through out the cell whereas in Hip1Si cells, most of the GFP-HIPPI was localized in the cytoplasm. Similar result was also obtained by immunocytochemistry in Hip1Si cells using anti-HIPPI antibody labeled with TRITC (Figure 4B). We further compared the extent of HIPPI in the cytoplasmic and nuclear fractions of the cell extract from GFP-Hippi expressing HeLa cells ('Hippi') and HeLa cells with knocked down HIP-1 (Hip1SiHi) using western blot analysis. Result of a typical experiment is shown in Figure 4C, panel I. The average IOD of two independent experiments is shown graphically in the panel II of Figure 4C. The result showed that nuclear content of HIPPI in Hip1SiHi cells, where endogenous HIP-1 had been knocked down, was reduced (27 ± 3%) compared to HeLa cells expressing GFP-HIPPI (58 ± 11%). The reduction was statistically significant ($P = 0.009$). These results indicated that HIP-1 might be involved in transporting its partner HIPPI from the cytoplasm to the nucleus.

We argued that if the endogenous HIP-1 was necessary to translocate exogenous GFP-HIPPI into the nucleus, the amount of HIP-1 should also increase in the nuclei of GFP-Hippi expressing cells. Western blot analysis was carried out to compare the amount of HIP-1 in the nuclear and cytoplasmic fractions of HeLa cells expressing GFP-Hippi ('Hippi') and the parental HeLa cells (HeLa). Result of a typical experiment is shown in Figure 4D, panel I. The average IOD of two independent experiments graphically shown in Figure 4D, panel II, indicates that the amount of HIP-1 in the nuclear fractions was significantly ($P = 0.04$) increased in GFP-Hippi expressing cells (46 ± 6%) compared to that obtained in HeLa cells (32 ± 6%). This was further tested by cytochemistry using either FITC (for endogenous HIP-1 detection in HeLa) or TRITC (for detection of endogenous HIP-1 in presence of GFP-HIPPI) labeled anti HIP-1 antibody (Figure 4E and F, respectively) in HeLa and GFP-Hippi expressing HeLa cells. These results showed that in the presence of GFP-HIPPI, excess amount of endogenous HIP-1 could be detected in the nucleus indicating that HIP-1 was translocated into the nucleus together with HIPPI as shown in Figure 4C. To investigate the role of different domains of HIP-1 in the translocation process of HIPPI, we co-expressed GFP-Hippi along with full-length Hip-1, Hip-1 N-terminus (1–258 aa) and pDED of Hip-1 (410–491 aa) cloned in DsRed in HeLa cells and observed under confocal microscope. It is to be noted that neither of the fragments namely N-terminal and pDED of HIP-1 contains the nuclear localization signals (amino acid positions 996–1009) (6). When GFP-Hippi was co-expressed with exogenous DsRed-Hip-1, the proteins co-localize and are present through out the cell (Supplementary Figure S1, panels I and IV). When GFP-Hippi was co-transfected with DsRed-Hip-1N or DsRed-Hip-1P, the nuclear localization of HIPPI was reduced (Supplementary Figure S1, panels II and III). However the extent of co-localization was much higher in cells co-expressing GFP-Hippi and DsRed-Hip-1P compared to GFP-Hippi and DsRed-Hip-1N (Supplementary Figure S1, panels V and VI). This result was similar to that published earlier showing HIPPI mainly interacted with the pDED of HIP-1 (1). This result also indicates that full length HIP-1 containing the nuclear localization signal is possibly necessary to translocate HIPPI into the nucleus.

HIPPI requires HIP-1 for nuclear translocation and transcriptional regulation of caspase-1 in Neuro2A cells

We investigated the effect of HIP-1 on the nuclear distribution of endogenous HIPPI and its subsequent regulation of caspase-1 expression, as described above with HeLa cells. To exclude the possibility of any cell line specific event related to the above observations, we first rechecked the role of HIP-1 in Neuro2A cells having endogenous HIP-1 and HIPPI (2). We knocked down endogenous HIP-1 in Neuro2A cells by Hip1Si (specific siRNA designed for human Hip-1 gene, see 'Materials and Methods' section). The human specific siRNA was able to down regulate the mouse HIP-1 (Figure 5A, designated as N2a Hip1Si). We further generated Neuro2A cells stably expressing the exogenous wild type Hip-1 (Figure 5A, denoted by N2aHip1), NLS mutant of Hip-1 (R1005E, designated by N2a1005E) and lipid-binding domain mutant of Hip-1 (K58E, designated by N2a58E) cloned in pcDNA3 (see 'Materials and Methods' section for details). Expression of endogenous HIP-1, exogenous HIP-1 and the two mutants are shown in Figure 5A, top panel. Average IOD of the protein bands obtained in independent experiments are shown in Figure 5B. Sub-cellular distribution of HIPPI in these cells was determined by western blot analysis. Result showed that proportion of nuclear HIPPI in the parental Neuro2A cells (N2a) was (0.45 ± 0.04) and reduced to (0.24 ± 0.01) in N2a Hip1Si cells. This decrease was statistically significant ($P = 0.02$, $n = 2$). Similarly, the cytoplasmic fraction of endogenous HIPPI was increased significantly in HIP-1 knocked down cells compared to that obtained in the parental Neuro2A cells (Figure 5C and D). Exogenous expression of wild type HIP-1 increased the nuclear fractions of HIPPI slightly but the increase was not statistically significant. However, exogenous expression of the NLS mutant (1005E) of HIP-1 showed significant ($P = 0.0006$, $n = 3$) accumulation of HIPPI in the cytoplasm as expected (Figure 5E and F). In this case, the nuclear fraction of HIPPI decreased from (0.47 ± 0.015) in N2a Hip1 cells to (0.31 ± 0.04) in cells expressing NLS mutant of HIP-1 (N2a1005E). Expression of Caspase-1 in the above cells as revealed by western blot also correlated with this observation. HIP-1 knocked down Neuro2A cells showed significantly ($P = 0.001$, $n = 2$) decreased expression of caspase-1 (Figure 5G and H) while cells over expressing wild type HIP-1 showed increase of the same ($P = 0.0002$, $n = 3$). Moreover, caspase-1 expression was decreased significantly ($P = 0.002$, $n = 3$) in N2a1005E cells compared to the parental Neuro2A cells. Caspase-1 expression in N2a 58E cells did not change significantly in comparison to that of Neuro2A cells ($P = 0.13$, $n = 2$). This result shows that HIP-1,

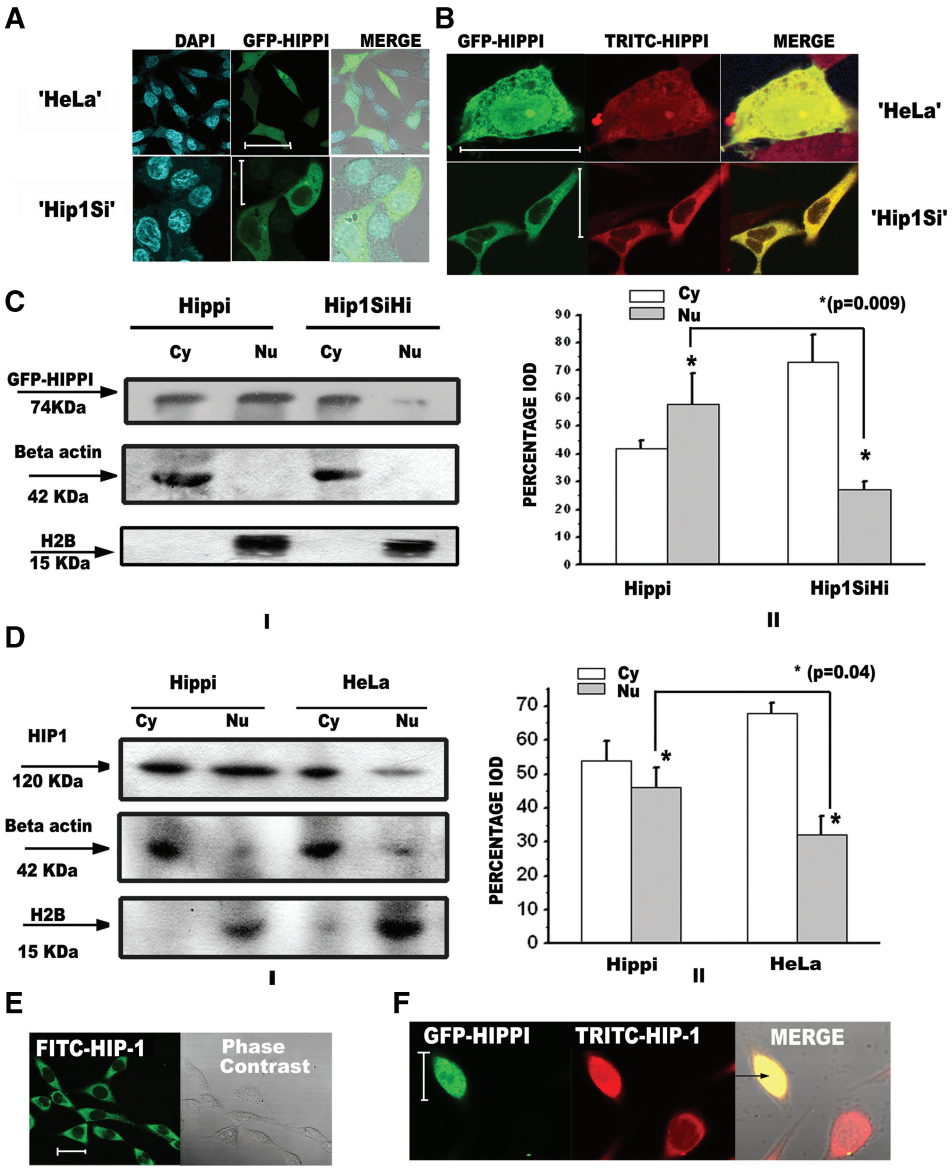

Figure 4. HIP-1 assists HIPPI for translocation into the nucleus from cytoplasm. (**A**) Representative photographs showing the localization of exogenous GFP-HIPPI in HeLa cells (upper panel) and in 'Hip1Si' cells (lower panel) taken using confocal microscope. Nuclei were visualized after staining cells with DAPI. White bar represents the dimension of a single cell (50 μm). (**B**) Immunocytochemistry for detection of exogenous GFP-HIPPI in HeLa and Hip1Si cells (HeLa cells stably transfected with HipSi, see text for details). HIPPI was immunostained with TRITC (Red) labeled secondary antibody. Green fluorescence signal of the GFP tag and red fluorescence signal of TRITC co localized in HeLa (upper panel) and in 'Hip1Si' (lower panel) (**C**) Western blot analysis for detection of cytoplasmic and nuclear fractions of GFP-HIPPI. HeLa cells expressing GFP-HIPPI is designated as 'Hippi' and that of HIP-1 knocked down HeLa cells is designated as 'Hip1SiHi'. Panel I: Upper panel shows the distribution of 74 kDa band corresponding to GFP–HIPPI in nuclear and cytoplasmic fractions of 'Hippi' and 'Hip1SiHi' cells. Middle panel shows the 42 kDa band corresponding to beta actin protein used as loading control for cytoplasmic extracts. Lowermost panels represent the 15 kDa band corresponding to H2B used as loading control for nuclear extract. Panel II: Bar diagrams showing fractions of GFP-HIPPI (expressed as percentage) in the cytoplasm (white bars) and nucleus (grey bars) obtained in 3 independent experiments using GFP-Hippi expressing HeLa cells (Hippi) and HIP-1 knocked down cells (Hip1SiHi). IODs obtained in each fraction were normalized by the IOD values obtained with anti beta actin (cytoplasmic) or H2B (nuclear) antibodies. Proportion of proteins in the cytoplasm and nucleus was determined by dividing the corresponding normalized IOD in cytoplasm and nucleus with the total IOD in the two compartments. The *P*-value indicates significant difference of GFP-HIPPI localization in nuclei of 'Hippi' and 'Hip1SiHi' cells. (**D**) Western blot analysis for the detection of cytoplasmic and nuclear fractions of endogenous HIP-1 in 'Hippi' and 'HeLa' cells. Panel I: Upper panel represents the 120 kDa band corresponding to HIP-1 protein present in nuclear and cytoplasmic fractions of 'Hippi' and parental HeLa cells. Middle panel shows the 42 kDa band corresponding to beta actin used as loading control for cytoplasmic extracts. Lowermost panels represent the 15 kDa band corresponding to H2B used as loading control for nuclear extract. Panel II: Histograms showing average ($n = 3$) of relative IOD (expressed as percentage) of bands obtained by western blot analysis with anti HIP-1 antibody determined as described in (C) above. Level of significance ($^*P = 0.04$, $n = 3$) is also shown in the figure. (**E**) Immunocytochemistry for the localization of endogenous HIP-1 in HeLa cells using anti HIP-1 antibody labeled with FITC (green). (**F**) Immunocytochemistry showing co-localization of GFP-HIPPI with endogenous TRITC labeled HIP-1 in GFP-Hippi transfected HeLa cells.

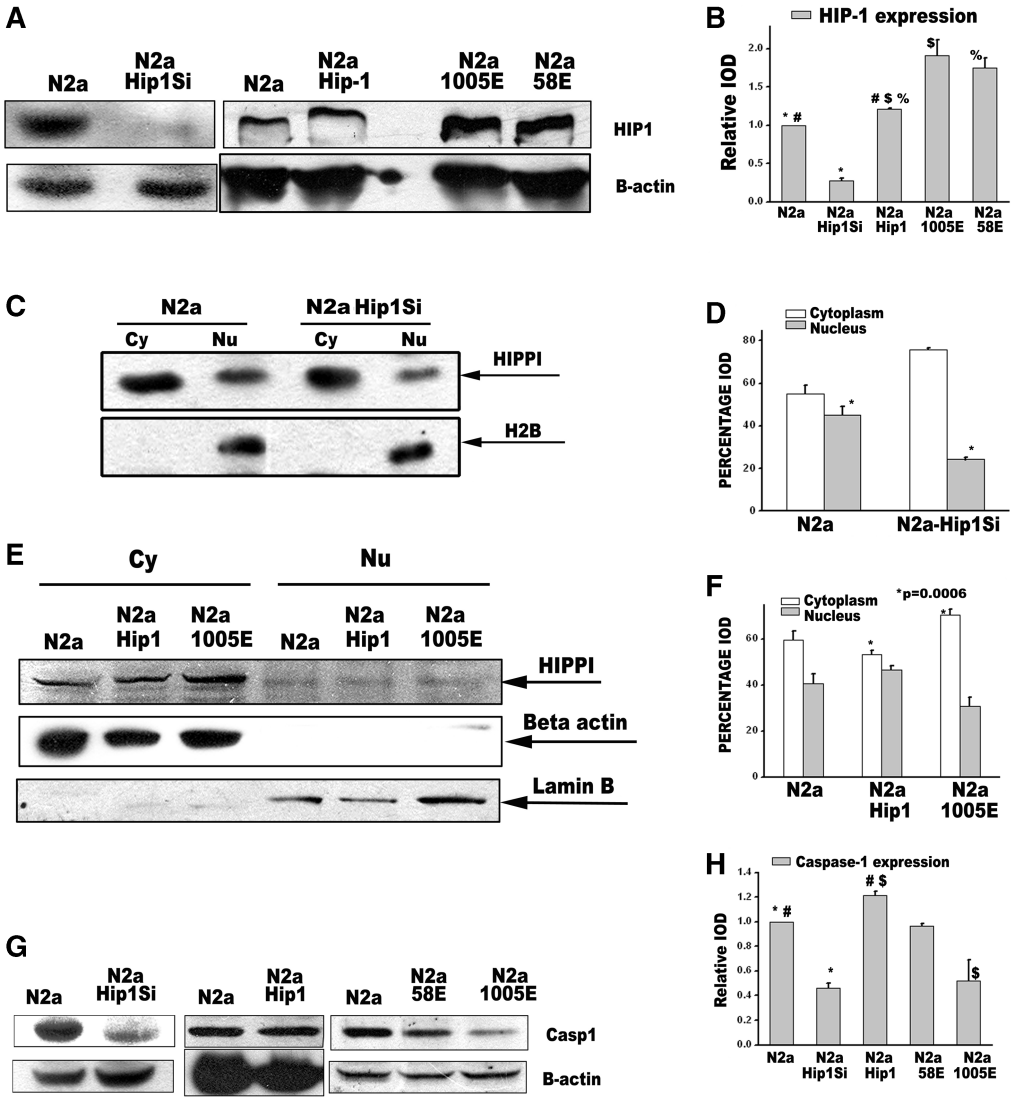

Figure 5. Involvement of HIP-1 and its mutants in transport of HIPPI into the nucleus and alteration of caspase-1 expression in Neuro2A cells. (**A**) Western blot analysis with total cell extracts from Neuro2A cells ('N2a'), HIP-1 knocked down Neuro2A cells ('N2a Hip1Si') and Neuro2A cells over expressing wild type pcDNA3-Hip-1 ('N2a Hip1'), NLS mutant ('N2a 1005E') and lipid-binding domain mutant of Hip-1 ('N2a 58E'). Both the NLS mutant and the lipid-binding domain mutant are cloned in pcDNA3. Upper panel shows the band corresponding to 120 kDa HIP-1. Lower panel shows the 42 kDa band of beta actin (B-actin) as loading control. (**B**) The bar diagram represents the mean IOD ($n = 2$) of bands obtained by western blot analysis with anti HIP-1 antibody and normalized by the IOD values obtained with anti beta actin antibody. Level of significance are $^{*}P = 0.002$, $^{\#}P = 0.001$, $^{\$}P = 0.04$, $^{\%}P = 0.03$. (**C**) Western blot analysis for cytoplasmic (Cy) and nuclear (Nu) protein fractions of 'N2a' and 'N2a-Hip1Si' cells. Upper panel shows the 49 kDa band corresponding to endogenous HIPPI. Lower panel represents the 15 kDa band of H2B as loading control for nuclear proteins. (**D**) Histogram representing the average ($n = 2$) of normalized IOD of bands corresponding to nuclear (grey bars) and cytoplasmic (white bars) fractions of HIPPI. Proportions of HIPPI in different cellular compartments were determined as described in the legend 4C. Level of significance is $^{*}P = 0.02$. (**E**) Western blot analysis for detection of cytoplasmic and nuclear fractions of HIPPI in the parental Neuro2A cells (N2a), Neuro2A cells stably transfected with pcDNA3-Hip-1 (N2aHip1) and Neuro2A cells stably transfected with pcDNA3-Hip-1 with mutation at the NLS (N2a1005E). Upper panel shows the 49 kDa band corresponding to endogenous HIPPI. Middle panel indicates cytoplasmic loading control beta actin (42 kDa). Lower panel indicates the 66 kDa band of Lamin B as loading control for nuclear protein. (**F**) Bar diagram showing the average ($n = 3$) fractions of endogenous HIPPI in the cytoplasm and nucleus in different cells as described in the legend of (E) above. Proportions of HIPPI were calculated as described in the legend of Figure 4C. Level of significance ($^{*}P = 0.0006$) is also shown in the figure. (**G**) Effect of HIP-1 and its mutants on the caspase-1 expressions in the parental Neuro2A cells (N2a), Neuro2A cells expressing stably Hip1Si (N2aHip1Si), wild type Hip-1 cloned in pcDNA3 (N2aHip1), pcDNA3-Hip-1 with mutations in lipid-binding domain (N2a58E) and NLS (N2a1005E). In the upper panel the 45 kDa bands correspond to pro-caspase-1. Lower panel shows the loading control beta actin (42 kDa). (**H**) The bar diagram shows the mean ($n = 3$) relative expression of caspase-1 in indifferent cells described in G above. IOD value of the caspas-1 specific band of the parental Neuro2A cells was normalized with the loading control beta actin and was considered to be 1. $^{*}P = 0.0027$, $^{\#}P = 0.0002$, $^{\$}P = 0.002$.

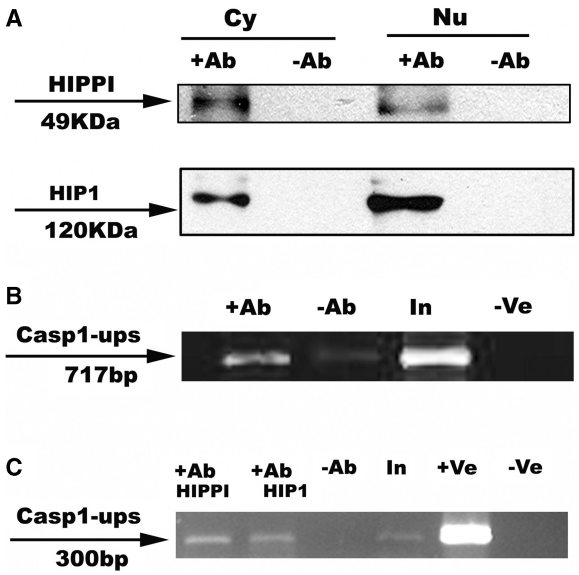

Figure 6. Interaction of HIPPI with HIP-1 in cytoplasm and nucleus and subsequent interaction of the complex with caspase-1 promoter *in vivo*. (**A**) Interaction of HIP-1 with HIPPI in cytoplasm and nucleus. Cytoplasmic (denoted by Cy) and nuclear (denoted by Nu) fractions of the cell extract were separately immunoprecipitated with anti HIP-1 antibody, transferred to membrane and detected with anti HIPPI antibody. Upper panel shows the bands corresponding to the endogenous HIPPI (49 kDa), while the lower panel represents the HIP-1 (120 kDa). Lanes indicated as +Ab show the result when the cell extracts were treated with anti HIP-1 antibody while −Ab lanes show the result without anti HIP-1 anti body (only IgG). (**B**) *In vivo* interactions of endogenous HIPPI with the caspase-1 putative promoter sequences in ChIP assay with K562 cells. PCR amplification was carried out using caspase-1 upstream 717 bp (−700 to +17) sequence specific primers from immuoprecipitated DNA-protein complex using anti-HIPPI antibody. Lanes +Ab: PCR was carried out with immunoprecipitated DNA-protein complex using anti-HIPPI antibody. PCR was also carried out with chromatin prepared from the same cell extract using only Rabbit IgG secondary antibody but in absence of anti HIPPI antibody (lane: −Ab). Lane In shows the result when PCR was carried out with DNA isolated from K562 cells. Lane −ve shows the result when PCR was carried out where no template was added. (**C**) *In vivo* interactions of HIP-1 with caspase-1 putative promoter sequence by re-ChIP assay in HeLa cells expressing GFP-Hippi. Precipitated chromatin is PCR amplified using caspase-1 promoter 300 bp (−283 to +17) specific primers. Lane +Ab 'HIPPI': PCR amplification was carried out using chromatin immunoprecipitated by anti HIPPI antibody. Lane +Ab 'HIP1': PCR amplification was carried out using chromatin re-immunoprecipitated by anti HIP-1 antibody. Lane −Ab: PCR amplification was carried out using chromatin immunoprecipitated by IgG alone. Lane In: PCR amplification was carried out using DNA isolated from GFP-Hippi expressing HeLa cells. Lane +ve: PCR amplification was carried out using a definite template of Caspase-1 promoter. Lane −ve: PCR amplification was carried out without adding any template.

specifically the NLS of HIP-1 is necessary to translocate HIPPI into the nucleus and regulate the expression of caspase-1.

Similar to what have been shown in HeLa cells with knocked down HIP-1, cytochemistry of endogenous HIPPI in HIP-1 knocked down Neuro2A cells revealed that presence of endogenous HIPPI in nucleus was also reduced compared to parental Neuro2A cells (Figure S2).

In vivo interaction of HIP-1-HIPPI heterodimer with caspase-1 promoter

To address whether HIPPI-HIP-1 heterodimer was present in the nucleus, Neuro2A cells were fractionated and subjected to immunoprecipitation using anti HIP-1 antibody. Western blot analysis using anti-HIPPI antibody showed that HIPPI was co-immunoprecipitated with HIP-1 from both cytoplasmic and nuclear fractions indicating the presence of the heterodimer in both the compartments (Figure 6A). To test if endogenous HIPPI interacted with the caspase-1 promoter *in vivo*, we have used K562 cells where both HIPPI as well as HIP-1 were substantially expressed as opposed to HeLa where the expression of endogenous HIPPI was lacking (2). Chromatin immunoprecipitation with anti HIPPI antibody and detection of the promoter sequence of caspase-1 by promoter-specific PCR primers indicated that endogenous HIPPI could interact with the caspase-1 promoter sequence (Figure 6B). Further, to check the association of HIP-1 with the caspase-1 promoter as a part of transcription complex with HIPPI, re-ChIP experiment was performed. GFP-Hippi expressing HeLa cells were subjected to chromatin immunoprecipitation with anti HIPPI antibody and the immunoprecipitated complex was further subjected to re-ChIP using anti HIP-1 antibody. The precipitated DNA was PCR amplified using sequence specific primers for caspase-1 promoter. As revealed from Figure 6C, HIP-1 was also found to be associated with caspase-1 promoter as a part of HIPPI-HIP-1 complex. Taking together, the results indicated that HIPPI-HIP-1 heterodimer could interact with the promoter of caspase-1 *in vivo*.

DISCUSSION

To identify the specific amino acid of HIPPI that interacts with caspase-1 promoter sequence, we hypothesized on the basis of structural modeling of pDED-HIPPI that R393 of HIPPI residing at putative α4 helix of pDED-HIPPI might be involved in such interaction and tested the hypothesis. We also determined the role of HIP-1, the molecular partner of HIPPI, in the translocation of HIPPI into the nucleus, in a similar way to that has been observed for AR (6). Results presented in this manuscript showed that R393 of HIPPI was involved in its interaction with caspase-1 promoter sequence in cultured cells and regulated the transcription of caspase-1 gene. Mutant pDED-HIPPI was able to interact with HIP-1 and activated Caspase-8. Besides, HIP-1 was involved in translocation of HIPPI from cytoplasm to the nucleus. Finally, we show that HIPPI-HIP-1 heterodimer participates in the transcription regulation of caspase-1 gene.

Death effecter domain (DED) containing proteins are known to participate in diverse cellular functions including apoptosis through receptor signalling (18,19). Other DED containing proteins namely, DEDD has been reported to regulate the transcription by RNA polymerase I (20,21). We have shown earlier that the expression of caspase-1 gene is increased in GFP-Hippi

expressing HeLa and Neuro2A cells. HIPPI directly interacts with the putative promoter of caspase-1, especially to the motif 5′-AAAGACATG-3′ (−101 to −93) present at the promoter sequence of caspase-1. HIPPI also binds to the putative promoter sequences of caspase-8 and caspase-10 where similar motifs are present (2,4,5). Our modelling studies revealed that the mutation R393E alters the local surface as well as the charge distribution but the overall conformation of the domain remains unperturbed (RMSD of R393 and E393 for Cα superposition = 0.024A°) (Figure 1). We further showed experimentally that the mutation of R393E of pDED-HIPPI decreased caspase-1 expression (Figure 2F) and abolished/decreased the binding of pDED-HIPPI to caspase-1 promoter in HeLa cells (Figures 2H). It has been shown earlier that K409 at the helix 5 of pDED-HIPPI is required for its interaction with HIP-1 and apoptosis induction (1), while we showed that the putative α4 helix of pDED of HIPPI was involved in the transcription regulation. Mutation R393E did neither alter the ability to interact with the endogenous HIP-1 (Figures 2C) nor the ability to activate caspase-8 and apoptosis (Figure 2G). HIPPI has been shown to induce apoptosis in co-operation with HIP-1 (1). Contradictory findings that HIP-1 may act as a prosurvival/antiapoptotic (22–25) or proapoptotic protein (1,2,26,27) depending on its interaction with other partner and reviewed recently (28). Our result shows the involvement of the specific amino acid R393 of HIPP1 for its interaction with specific DNA sequence and transcription regulation of caspase-1. However, mutation R393E of p DED-HIPPI did neither alter its ability to interact with HIP-1 nor apoptosis induction. The ability to regulate the transcription of caspase-1 and apoptosis by HIPPI thus resides in two different locations namely at α5 helix and α4 helix of pDED-HIPPI.

HIP-1 has recently been shown to enhance the transcription of AR-responsive genes by translocating AR to the nucleus in response to androgen. Furthermore, HIP-1 also acts as a co-activator for estrogen and glucocorticoid receptors. HIP-1 harbours NLS at its C-terminal (amino acid positions 996–1009) and a point mutation (R1005E) resulting in reduction of nuclear localization. HIP-1 is also known to reduce the rate of degradation of AR (6). Initial indirect evidence that similar mechanism is also involved in caspase-1 regulation by HIPPI has been provided earlier. Involvement of HIP-1 in the expression of caspase-1 is inferred indirectly from the result obtained in cells co-expressing *HTT* exon1, containing 16 CAG repeats tagged with DsRed, together with GFP-Hippi in HeLa cells. Over expression of N-terminal HTT with 16Q (coded by exon-1 of *HTT*) decreases the expression of caspase-1 in comparison to that obtained in HeLa cells expressing GFP-Hippi only (28). It has been argued that in presence of excess wild type HTT, endogenous HIP-1 preferentially interacts with it, decreasing freely available HIP-1 and thus also the availability of HIPPI-HIP-1 heterodimer (1,2). In turn this might lead to less HIPPI in the nucleus and reduces the expression of caspase-1 (2,28). Several lines of evidences provided in this manuscript further showed that full length HIP-1 is necessary for the relocation of cytoplasmic HIPPI into the nucleus. First, in the presence of exogenous HIPPI and endogenous HIP-1 in HeLa cells, the extent of nuclear fractions of HIPPI as well as HIP-1 was increased significantly (Figure 4D) and the expression of caspase-1 was also elevated under such condition (2). Secondly, in HeLa cells with knocked down HIP-1, the extents of nuclear fraction of exogenous HIPPI as well as the expression of caspase-1 were decreased (Figures 4A, B, C, and 3A). Similar result was also obtained with pDED of HIPPI (data not shown). Thirdly, knocked down endogenous HIP-1 in Neuro2A cells decreased the extent of nuclear fractions of endogenous HIPPI (Figure 5C and D) and in such condition the expression of caspase-1 was reduced (Figure 5G and H). Finally, exogenous expression of HIP-1 significantly increased the expression of caspase-1. The exogenous expression of NLS mutant of HIP-1 resulted in cytoplasmic accumulation of HIPPI thereby decreasing expression of caspase-1. In the presence of exogenous mutant HIP-1, possibly some fractions of endogenous HIPPI remained in the cytoplasm by interacting with mutant HIP-1 and thus reduced the caspase-1 expression. Role of endogenous HIPPI in the regulation of caspase-1 expression was evident from the HIP-1 knocked down cells where nuclear fraction of endogenous HIPPI was reduced. As expected in such condition, the expression of caspase-1 was also reduced. In addition, using K562 cells, where endogenous HIP-1 and HIPPI were present, we observed that HIPPI could bind to the caspase-1 promoter *in vivo* (Figure 6B).

To identify whether HIPPI-HIP-1 heterodimer directly interacts with DNA, we first observed that HIPPI-HIP-1 complex was present in cytoplasm as well as in the nucleus (Figure 6A). In re-ChIP assay using GFP-Hippi expressing HeLa cells where anti HIPPI antibody was used initially to pull down DNA-protein complex and then the immunoprecipitated complex was further pulled down by anti HIP-1 antibody, we could detect caspase-1 upstream sequence (Figure 6C). This result showed that HIPPI-HIP-1 was present in the transcription complex. We have earlier shown that RNA polymerase II is also present in the HIPPI-DNA complex (4). Taking together, this result showed that HIPPI-HIP-1 interacted with the promoter of caspase-1 and formed active transcriptional complex. It remains to be found out whether HIP-1 also directly interacts with DNA. Role of other interacting partners of HIPPI, namely RYBP (29) and BAR (30) in the transcription regulation by HIPPI is also elusive.

In summary, we showed that R393 of HIPPI at the α4 helix of pDED-HIPPI was involved in the interaction with DNA (this study) and a different interface formed by the amino acids at helix α5 participated in the interaction of pDED-HIPPI with HIP-1 and apoptosis regulation (1). We provided a second example (other than AR), where HIP-1, an endocytic protein is involved in a nuclear function. Significance of this result in connection with Huntington's disease is not known at present. However, result presented in this communication together with our earlier published work (2,4,5,28) established HIPPI as a transcription regulator for caspase-1 gene. It would be of immense interest to find out other genes, including

those altered in Huntington's disease that may be regulated by HIPPI.

SUPPLEMENTARY DATA

Supplementary Data are available at NAR Online.

ACKNOWLEDGEMENT

The authors acknowledge Dr Swasti Roychoudhuri, Crystallography and Molecular Biology Division and Structural Genomics Section, Saha Institute of Nuclear Physics, for his help in confocal microscopic experiments. They also acknowledge Mr Utpal Basu and Mr Saikat Mukherjee, Crystallography and Molecular Biology Division, Saha Institute of Nuclear Physics for their technical support.

FUNDING

Institutional grant from the Department of Atomic Energy, Government of India.

Conflict of interest statement. None declared.

REFERENCES

1. Gervais,F.G., Singaraja,R., Xanthoudakis,S., Gutekunst,C.A., Leavitt,B.R., Metzler,M., Hackam,A.S., Tam,J., Vaillancourt,J.P., Houtzager,V. *et al*. (2002) Recruitment and activation of caspase-8 by the Huntingtin-interacting protein Hip-1 and a novel partner Hippi. *Nat. Cell Biol.*, **4**, 95–105.
2. Majumder,P., Chattopadhyay,B., Mazumder,A., Das,P. and Bhattacharyya,N.P. (2006) Induction of apoptosis in cells expressing exogenous Hippi, a molecular partner of huntingtin-interacting protein Hip1. *Neurobiol. Dis.*, **22**, 242–256.
3. Kalchman,M.A., Koide,H.B., McCutcheon,K., Graham,R.K., Nichol,K., Nishiyama,K., Kazemi-Esfarjani,P., Lynn,F.C., Wellington,C., Metzler,M. *et al*. (1997) HIP1, a human homologue of S. cerevisiae Sla2p, interacts with membrane-associated huntingtin in the brain. *Nat. Genet.*, **16**, 44–53.
4. Majumder,P., Chattopadhyay,B., Sukanya,S., Ray,T., Banerjee,M., Mukhopadhyay,D. and Bhattacharyya,N.P. (2007) Interaction of HIPPI with putative promoter sequence of caspase-1 in vitro and in vivo. *Biochem. Biophys. Res. Commun.*, **353**, 80–85.
5. Majumder,P., Choudhury,A., Banerjee,M., Lahiri,A. and Bhattacharyya,N.P. (2007) Interactions of HIPPI, a molecular partner of Huntingtin interacting protein HIP1, with the specific motif present at the putative promoter sequence of the caspase-1, caspase-8 and caspase-10 genes. *FEBS J.*, **274**, 3886–3899.
6. Mills,I.G., Gaughan,L., Robson,C., Ross,T., McCracken,S., Kelly,J. and Neal,D.E. (2005) Huntingtin interacting protein 1 modulates the transcriptional activity of nuclear hormone receptors. *J. Cell Biol.*, **170**, 191–200.
7. Hyun,T.S. and Ross,T.S. (2004) HIP1: trafficking roles and regulation of tumorigenesis. *Trends Mol. Med.*, **10**, 194–199.
8. Vecchi,M. and Di Fiore,P.P. (2005) It's HIP to be a hub: new trends for old-fashioned proteins. *J. Cell Biol.*, **170**, 169–171.
9. Pilecka,I., Banach-Orlowska,M. and Miaczynska,M. (2007) Nuclear functions of endocytic proteins. *Eur. J. Cell Biol.*, **86**, 533–547.
10. Marti-Renom,M.A., Stuart,A.C., Fiser,A., Sanchez,R., Melo,F. and Sali,A. (2000) Comparative protein structure modeling of genes and genomes. *Annu. Rev. Biophys. Biomol. Struct.*, **29**, 291–325.
11. Guda,C., Scheeff,E.D., Bourne,P.E. and Shindyalov,I.N. (2001) A new algorithm for the alignment of multiple protein structures using Monte Carlo optimization. *Pac. Symp. Biocomput.*, **6**, 275–286.
12. Pearl,F., Todd,A., Sillitoe,I., Dibley,M., Redfern,O., Lewis,T., Bennett,C., Marsden,R., Grant,A., Lee,D. *et al*. (2005) The CATH Domain Structure Database and related resources Gene3D and DHS provide comprehensive domain family information for genome analysis. *Nucleic Acids Res.*, **33**, D247–D251.
13. Berman,H.M., Westbrook,J., Feng,Z., Gilliland,G., Bhat,T.N., Weissig,H., Shindyalov,I.N. and Bourne,P.E. (2000) The Protein Data Bank. *Nucleic Acids Res.*, **28**, 235–242.
14. Nicholls,A., Sharp,K.A. and Honig,B. (1991) Protein folding and association: insights from the interfacial and thermodynamic properties of hydrocarbons. *Proteins*, **11**, 281–296.
15. Niu,Q. and Ybe,J.A. (2008) Crystal structure at 2.8 A of Huntingtin-interacting protein 1 (HIP1) coiled-coil domain reveals a charged surface suitable for HIP1 protein interactor (HIPPI). *J. Mol. Biol.*, **375**, 1197–1205.
16. Li,F.Y., Jeffrey,P.D., Yu,J.W. and Shi,Y. (2006) Crystal structure of a viral FLIP: insights into FLIP-mediated inhibition of death receptor signaling. *J. Biol. Chem.*, **281**, 2960–2968.
17. Thore,S., Mauxion,F., Seraphin,B. and Suck,D. (2003) X-ray structure and activity of the yeast Pop2 protein: a nuclease subunit of the mRNA deadenylase complex. *EMBO Rep.*, **4**, 1150–1155.
18. Ashkenazi,A. and Dixit,V.M. (1998) Death receptors: signaling and modulation. *Science*, **281**, 1305–1308.
19. Weber,C.H. and Vincenz,C. (2001) The death domain superfamily: a tale of two interfaces? *Trends Biochem. Sci.*, **26**, 475–481.
20. Schickling,O., Stegh,A.H., Byrd,J. and Peter,M.E. (2001) Nuclear localization of DEDD leads to caspase-6 activation through its death effector domain and inhibition of RNA polymerase I dependent transcription. *Cell Death Differ.*, **8**, 1157–1168.
21. Zhan,Y., Hegde,R., Srinivasula,S.M., Fernandes-Alnemri,T. and Alnemri,E.S. (2002) Death effector domain-containing proteins DEDD and FLAME-3 form nuclear complexes with the TFIIIC102 subunit of human transcription factor IIIC. *Cell Death Differ.*, **9**, 439–447.
22. Bradley,S.V., Hyun,T.S., Oravecz-Wilson,K.I., Li,L., Waldorff,E.I., Ermilov,A.N., Goldstein,S.A., Zhang,C.X., Drubin,D.G., Varela,K. *et al*. (2007) Degenerative phenotypes caused by the combined deficiency of murine HIP1 and HIP1r are rescued by human HIP1. *Hum. Mol. Genet.*, **16**, 1279–1292.
23. Khatchadourian,K., Smith,C.E., Metzler,M., Gregory,M., Hayden,M.R., Cyr,D.G. and Hermo,L. (2007) Structural abnormalities in spermatids together with reduced sperm counts and motility underlie the reproductive defect in HIP1-/- mice. *Mol. Reprod. Dev.*, **74**, 341–359.
24. Bradley,S.V., Holland,E.C., Liu,G.Y., Thomas,D., Hyun,T.S. and Ross,T.S. (2007) Huntingtin interacting protein 1 is a novel brain tumor marker that associates with epidermal growth factor receptor. *Cancer Res.*, **67**, 3609–3615.
25. Hyun,T.S., Rao,D.S., Saint-Dic,D., Michael,L.E., Kumar,P.D., Bradley,S.V., Mizukami,I.F., Oravecz-Wilson,K.I. and Ross,T.S. (2004) HIP1 and HIP1r stabilize receptor tyrosine kinases and bind 3-phosphoinositides via epsin N-terminal homology domains. *J. Biol. Chem.*, **279**, 14294–14306.
26. Choi,S.A., Kim,S.J. and Chung,K.C. (2006) Huntingtin-interacting protein 1-mediated neuronal cell death occurs through intrinsic apoptotic pathways and mitochondrial alterations. *FEBS Lett.*, **580**, 5275–5282.
27. Kang,J.E., Choi,S.A., Park,J.B. and Chung,K.C. (2005) Regulation of the proapoptotic activity of huntingtin interacting protein 1 by Dyrk1 and caspase-3 in hippocampal neuroprogenitor cells. *J. Neurosci. Res.*, **81**, 62–72.
28. Bhattacharyya,N.P., Banerjee,M. and Majumder,P. (2008) Huntington's disease: roles of huntingtin-interacting protein 1 (HIP-1) and its molecular partner HIPPI in the regulation of apoptosis and transcription. *FEBS J.*, **275**, 4271–4279.
29. Stanton,S.E., Blanck,J.K., Locker,J. and Schreiber-Agus,N. (2007) Rybp interacts with Hippi and enhances Hippi-mediated apoptosis. *Apoptosis*, **12**, 2197–2206.
30. Roth,W., Kermer,P., Krajewska,M., Welsh,K., Davis,S., Krajewski,S. and Reed,J.C. (2003) Bifunctional apoptosis inhibitor (BAR) protects neurons from diverse cell death pathways. *Cell Death Differ.*, **10**, 1178–1187.